Working Memory Processes Are Mediated by Local and Long-range Synchronization of Alpha Oscillations

Maite Crespo-Garcia[1], Diego Pinal[1,2], Jose L. Cantero[1], Fernando Díaz[2], Montserrat Zurrón[2], and Mercedes Atienza[1]

Abstract

■ Different cortical dynamics of alpha oscillations (8–13 Hz) have been associated with increased working memory load, which have been mostly interpreted as a neural correlate of functional inhibition. This study aims at determining whether different manifestations of load-dependent amplitude and phase dynamics in the alpha band can coexist over different cortical regions. To address this question, we increased information load by manipulating the number and spatial configuration of domino spots. Time–frequency analysis of EEG source activity revealed (i) load-independent increases of both alpha power and interregional alpha-phase synchrony within task-irrelevant, posterior cortical regions and (ii) load-dependent decreases of alpha power over areas of the left pFC and bilateral posterior parietal cortex (PPC) preceded in time by load-dependent decreases of alpha-phase synchrony between the left pFC and the left PPC. The former results support the role of alpha oscillations in inhibiting irrelevant sensorimotor processing, whereas the latter likely reflect release of parietal task-relevant areas from top–down inhibition with load increase. This interpretation found further support in a significant latency shift of 15 msec from pFC to the PPC. Together, these results suggest that amplitude and phase alpha dynamics in both local and long-range cortical networks reflect different neural mechanisms of top–down control that might be crucial in mediating the different working memory processes. ■

INTRODUCTION

Living organisms are constantly interacting with a complex and dynamic environment. Their adaptive behaviors in response to new circumstances often rely on information that is no longer present, but temporarily represented in short-lasting neuronal traces. The ability to retain and manipulate this transient information, known as working memory (WM), is required for successful cognitive performance and is supported by a well-organized multicomponent system (Baddeley, 1998, 2002).

It is indisputable that all the WM processes require the involvement of neuronal mechanisms able to integrate information at different spatial scales in the absence of stimulation. Oscillatory synchrony seems to be a good candidate for such a purpose (e.g., Singer, 2009; Womelsdorf & Fries, 2007). Although human neuroelectric and neuromagnetic recordings have reported amplitude and phase modulations of local and long-range oscillatory activity in several frequency bands, apparent contradictory results of numerous studies do not allow clear conclusions regarding their functional role. The debate is particularly intense in relation to the contribution of alpha oscillations (8–13 Hz) to WM processes (Klimesch, Fellinger, & Freunberger, 2011; Palva & Palva, 2007, 2011; Klimesch, Sauseng, & Hanslmayr, 2007). Many studies have reported selective increases of alpha power over posterior cortical regions with increases in memory load and/or attentional demands (Haenschel et al., 2009; Scheeringa et al., 2009; Tuladhar et al., 2007; Busch & Herrmann, 2003; Cooper, Croft, Dominey, Burgess, & Gruzelier, 2003; Jensen, Gelfand, Kounios, & Lisman, 2002; Schack & Klimesch, 2002), whereas others have found the opposite result (Stipacek, Grabner, Neuper, Fink, & Neubauer, 2003; Gevins, Smith, McEvoy, & Yu, 1997; Gundel & Wilson, 1992). However, evidence suggests that these two patterns of results are not mutually exclusive and can be obtained within different alpha subbands over different cortical regions (Michels et al., 2010; Grimault et al., 2009; Meltzer et al., 2008; Michels, Moazami-Goudarzi, Jeanmonod, & Sarnthein, 2008; Sauseng, Klimesch, Doppelmayr, et al., 2005).

Studies in monkeys have revealed that alpha-generating mechanisms are located in different layers, depending on the level of cortical processing in the visual hierarchy (Bollimunta, Chen, Schroeder, & Ding, 2008), likely to support different functions (Mo, Schroeder, & Ding, 2011). Results from these studies suggest that visual processing is facilitated by concomitant increases of alpha power and neuronal firing in inferotemporal cortices (Mo et al., 2011) as well as by decreases of alpha power in occipital regions with visual attention (Bollimunta et al., 2008). These findings have two important implications: (i) both decreases and increases of alpha oscillatory

[1]University Pablo de Olavide, Seville, Spain, [2]University of Santiago de Compostela, Galicia, Spain

Journal of Cognitive Neuroscience 25:8, pp. 1343–1357
doi:10.1162/jocn_a_00379

activity may reflect enhanced neuronal excitability depending on the laminar profile of alpha organization and (ii) different alpha-generating mechanisms may act in parallel over different regions of the visual pathway to play different roles in WM processes. Accordingly, alpha power modulations in lower visual areas likely reflect different levels of neuronal excitability associated with either visual processing of the attended event or inhibition of unattended information (Klimesch et al., 2007; Kelly, Lalor, Reilly, & Foxe, 2006; Thut, Nietzel, Brandt, & Pascual-Leone, 2006; Sauseng, Klimesch, Doppelmayr, et al., 2005; Yamagishi et al., 2003; Jensen et al., 2002; Worden, Foxe, Wang, & Simpson, 2000; Vanni, Revonsuo, & Hari, 1997), whereas alpha in higher visual areas may play a role in amplifying the representation of task-relevant information (Mo et al., 2011; see also Palva & Palva, 2007, 2011; Grimault et al., 2009). These modulations of neuronal activity in posterior cortical regions are thought to derive from top–down control mechanisms in pFC (Zhang & Ding, 2010; Moore & Armstrong, 2003; Miller, Erickson, & Desimone, 1996). In line with this hypothesis, a few studies have found increases in the power of prefrontal alpha activity and/or in the strength of frontoparietal alpha coupling with increasing memory load and attentional demands (Palva, Kulashekhar, Hämäläinen, & Palva, 2011; Michels et al., 2010; Palva, Monto, Kulashekhar, & Palva, 2010; Grimault et al., 2009; Leiberg, Lutzenberger, & Kaiser, 2006; Sauseng, Klimesch, Doppelmayr, et al., 2005; Sauseng, Klimesch, Schabus, & Doppelmayr, 2005; Cooper et al., 2003; von Stein & Sarnthein, 2000).

Therefore, alpha oscillatory dynamics may contribute in different ways to both the peripheral and executive systems contemplated in the Baddeley's model: (i) by strengthening maintenance of stimulus representations through alpha decreases in task-relevant regions (although increases are also feasible), (ii) by suppressing distractor information through alpha increases in task-irrelevant regions, and (iii) by sending top–down control signals from different regions within pFC to the peripheral systems that could be either excitatory or inhibitory in nature. This study has a twofold objective: to determine whether these different manifestations of alpha activity can coexist and whether they are equally influenced by memory load.

To achieve these goals, we evaluated variations in the regional power and interregional phase of EEG alpha oscillatory activity at the source level while participants retained one domino piece that either contained two to three spots (low-load condition) or four to five spots (high-load condition). As information of a domino tile is integrated into one single object, it will be processed in the ventral stream. However, this processing is based on object features like spatial distribution of an increasing number of spots in the tile and consequently also requires the involvement of the parietal cortex (Fletcher et al., 1995; Roland, Gulyás, Seitz, Bohm, & Stone-Elander, 1990). If alpha power modulations, acting through different generating mechanisms (Bollimunta et al., 2008), reflect basic processes of WM function, different patterns of results are expected to coexist in lower and higher visual areas (Mo et al., 2011). These patterns would include load-induced decreases over task-relevant regions mainly affecting higher visual areas in the dorsal stream to maintain spatial distribution of spots, and load-induced increases over task-irrelevant regions mainly affecting lower visual areas in or around the parieto-occipital sulcus to protect visual processing from potential interference. If in addition, frontoparietal neural pathways communicating in the alpha band are partially responsible for the load-dependent alpha dynamics described above, alpha oscillations in these two regions not only should be highly synchronized but also activity in pFC is expected to drive alpha oscillations in the posterior parietal cortex (PPC).

After the retention period, participants were asked to identify among three domino tiles of the same level of complexity (e.g., similar number of spots) which one matched the sample domino. According to the two-factor model of WM function (Awh, Barton, & Vogel, 2007), increased information load may affect performance negatively not only because of increased number of spots but also because of increased similarity between sample and test items during the comparison stage. Consistent with this two-factor model, it has been suggested that the inferior intraparietal sulcus may determine the number of representations that can be stored, whereas the superior intraparietal sulcus and lateral occipital regions might be more related to the resolution of such representations (Anderson, Vogel, & Awh, 2011; Xu & Chun, 2006). To test whether the resolution component of WM is also mediated by modulations of alpha oscillations in the cortical regions mentioned above, trials were further split based on the degree of the sample–test similarity. According to predictions derived from the two-factor model, performance (hence alpha power) should be influenced by sample–test similarity mainly under high-load conditions in both the retention and retrieval periods, because domino tiles were more complex in this condition (i.e., four to five spots).

METHODS

Participants

Twenty-nine healthy volunteers (20 women, 20.5 ± 2.84 years) from the University of Santiago participated in this study. All participants, except for three, were right-handed as assessed by the Edinburgh Handedness Inventory (Oldfield, 1971). All of them had normal or corrected-to-normal vision, with no history of neurological or psychiatric disorders. They were instructed to abstain from drugs, alcohol, and caffeine the day prior to the experimental session. All participants gave their informed consent before the experimental session and were paid for their participation. The study was conducted according to the principles outlined

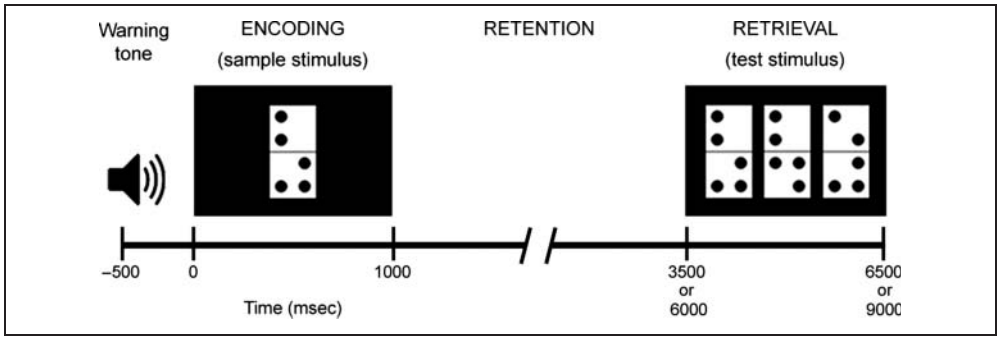

Figure 1. Schematic representation of the delayed match-to-sample (DMS) task. A warning auditory tone (1000 Hz, 50 msec) was followed, after 500 msec, by a sample domino tile for 1000 msec (encoding interval). After a delay of 2500 or 5000 msec (retention interval), participants were asked to identify the sample domino among three different tiles with the same load information. If no response was given, the test stimulus finished after 3000 msec.

in the Declaration of Helsinki and approved by the Ethical Committee at the University of Santiago.

Experimental Protocol

Participants performed the visuospatial delayed match-to-sample (DMS) task illustrated in Figure 1. Every trial began with a warning tone (1000 Hz, 50 msec) that alerted of the arrival of a sample stimulus (a domino tile present in the screen for 1000 msec) 500 msec later. After a time delay of either 2500 or 5000 msec, three test stimuli containing similar information load as the sample were presented for 3000 msec or until the participant's response. Participants were asked to identify the tile that matched the sample domino by pressing one of three response buttons as quickly and accurately as possible. A fixation cross was presented to reduce ocular movements during the retention period and during the 800-msec intertrial interval. We used a block design, in which different WM load conditions, low load (LL) and high load (HL), were presented in two consecutive blocks of 90 trials each. The LL block included dominoes with two or three spots, and the HL block grouped the dominoes containing four or five spots.

Behavioral Analysis

The effects of WM load on hit proportion and RTs were analyzed using paired-sample *t* tests, with the WM load condition as the within-subject factor (LL vs. HL). Hit proportion was computed as the number of correct responses from among all responses for each WM load condition. RTs were calculated for correct responses as the elapsed time between the test stimulus onset and the participant response.

The two-factor model of WM function states that more complex stimuli are also likely to result in larger sample–test similarity and hence in larger distractor interference during memory recognition (Awh et al., 2007). To test these hypotheses, we computed a dissimilarity index that takes into account differences in the number and position of spots between sample and test dominoes and next performed correlation analyses with RTs across trials as well as for the LL and HL trials separately. The dissimilarity index (DI) was defined as follows:

$$\mathrm{DI} = \left(|n - n_{\mathrm{test}}| \cdot 2 + \sum_{i=1}^{n} |\mathrm{displacement}_i| \right) / n$$

where n_{sample} is the number of spots in the sample domino and n_{test} denotes the number of spots in one of the two test domino tiles that differed from the sample domino. Differences in the number of spots between sample and test dominoes were multiplied by a factor of 2 because this type of change was easier to detect than a spot displacement. The $\mathrm{displacement}_i$ refers to the position difference of the spot i between sample and test (normalized Euclidean distance). This variable contemplates the fact that horizontal and vertical displacements are more difficult to identify than the diagonal ones. Finally, a mean dissimilarity index for each trial was obtained by averaging the dissimilarity indexes from the two-distractor domino tiles. In the example shown in Figure 1, the distractor dominoes included only one vertical displacement, so dissimilarity in the two cases would be 1/5, and the mean dissimilarity index would be 0.2. However, if one of the domino tiles would have included in its superior half two spots in the horizontal line (like the example shown in Figure 3A, for the HL condition), the change would have been easier to discriminate, and accordingly, the dissimilarity index for that particular tile would have been ≈0.28 ($\sqrt{2}/5$).

EEG Recordings and Signal Preprocessing

EEG activity was recorded from 49 active electrodes inserted in a cap (EasyCap GmbH) and placed in the standard positions of the International 10–10 system, including midline (AFz, Fz, FCz, Cz, CPz, Pz, Oz) and lateral (AF7, AF3, F7, F5, F3, FT9, FT7, FC3, FC1, T7, C5, C3, C1, TP9,

TP7, CP3, P9, P7, P3, PO7, O1, and their homologous) sensors. EEG data were nose-referenced but were later reformatted to the common average reference to diminish inflated synchronization values between neighbor EEG sites (Nunez et al., 1997). Horizontal and vertical ocular movements were monitored with pairs of electrodes placed above and below the right eye and 1 cm apart from the outer canthus of each eye. All electrode impedances were kept below 10 KΩ. Signals were filtered on-line with a 0.01–100 Hz analog bandpass and digitized at 500 Hz. EEG data were preprocessed with a digital bandpass filter from 0.5 to 70 Hz (12 dB/octave slope) and resampled to 250 Hz. To partially remove ocular and muscular artifacts, we applied the Infomax-independent component analysis algorithm as implemented in the Brain Vision Analyzer software (v.2 Brain Products GmbH). Remaining artifacts were rejected manually. EEG epochs were set from 1300 msec before sample stimulus onset to 1500 msec after test stimuli presentation. The first 500 msec were used as the baseline period to avoid the contribution of the activity elicited by the tone and to prevent expectation effects. For each participant, we selected the same number of trials (only correct responses) for the two load conditions (mean = 77; standard deviation = 7.4; minimum = 52). To isolate the non-phase-locked activity from the evoked components, the averaged ERP was subtracted from the total activity of each baseline-corrected individual trial.

Time–Frequency EEG Analysis

The FieldTrip toolbox (Oostenveld, Fries, Maris, & Schoffelen, 2011; fieldtrip.fcdonders.nl/) was used to calculate baseline-corrected time–frequency representations (TFR) of power across trials. We applied the multitaper method (Percival & Walden, 1993) to frequencies from 2 to 25 Hz, with identical resolution parameters as previously used in Jokisch and Jensen (2007) for the low-frequency range. The mean power of the baseline interval was subtracted from power values calculated within three different time intervals referring to the prestimulus and encoding interval (1500 msec following onset of the warning tone), retention (2500 msec following sample stimulus offset), and retrieval (1500 msec following test stimulus onset). These values were normalized, dividing them by the mean power of the baseline interval. Resulting TFRs were averaged over trials for each participant and for each condition of information load and resolution, separately.

Cortical Dynamics of EEG-alpha Sources Associated with WM Processes

Analyses at the Sensor Level

Increases/decreases of alpha power relative to baseline as well as influence of memory load and sample–test similarity were determined by applying the partial least squares (PLS) analysis. Here we used the PLScmd toolbox for Matlab, freely available at www.rotman-baycrest.on.ca/pls/source/. We performed a mean-centering approach on both evoked (phase-locked) and induced (non-phase-locked) activity separately, but results revealed that effects were only associated with the non-phase-locked components of EEG oscillations. Statistical significance was assessed by 10,000 permutations, and standard errors were estimated from 2000 bootstraps.

Additionally, regression analyses were performed at the individual level to determine the relationship between alpha oscillations within the time–frequency windows mentioned above and RTs for each condition of information load and sample–test similarity. Next, we compared the collection of beta coefficients to the value of zero using a one-sample *t* test. If results were significant in at least one of the two conditions, then paired *t* tests were computed at the group level to test for differences between conditions across time, frequency, and spatial dimensions. All these contrasts were repeated in consecutive time windows of 40 msec within the retention and retrieval periods. The maximum cluster mass statistic was applied to correct the family-wise error rate for all sensors and time–frequency points jointly (Nichols & Holmes, 2002), performing 1000 randomizations of the data and using the 95th quantile of the statistic distribution as a critical threshold ($\alpha = .05$).

Analyses at the Source Level

Cortical sources of EEG-alpha oscillations were estimated using multiple source beamformer. The beamformer is an adaptive spatial filter that estimates the amount of activity at any given location by minimizing contributions from all other source locations. The particular spatial filtering approach used here produces volumetric images of brain activity by dividing uniformly the entire brain into voxels of 5 mm. As beamforming assumes that sources in different parts of the brain are not temporally correlated, we applied an approach with multiple constraints to reduce the pernicious effect of correlated EEG sources (Dalal, Sekihara, & Nagarajan, 2006). To obtain the constrained locations, a dual-core beamformer method was first applied to identify the pairs of correlated EEG sources that coexist in each individual data set without a priori knowledge (Diwakar et al., 2011). To obtain the volumetric images of source activity, we used a realistic boundary element model (Oostenveld, Praamstra, Stegeman, & van Oosterom, 2001) based on a standard template (Colin27 T1-weighted averaged MRI) of the Montreal Neurological Institute (MNI).

The effect of load and/or sample–test similarity was also evaluated on the source activation maps. We first compared the interval of interest with the baseline period for each participant by applying a voxel-wise *t* test for independent samples on the source activation maps. In a second step, *t* statistic maps obtained from

all participants were entered into a one-sample t test at the group level to determine brain regions showing significant power increases within the interval of interest relative to the baseline. Additionally, a paired-sample t test was applied at the group level using individual t-statistic maps to determine cortical regions showing power modulations with either increasing memory load or increasing sample–test similarity. For all contrasts, the family-wise error rate was controlled by applying nonparametric permutation tests (1000) together with the suprathreshold maximum cluster mass statistic ($\alpha = .05$; Nichols & Holmes, 2002). Coordinates of voxels showing local maxima t statistics were transformed from the MNI space to the Talairach space (Talairach & Tournoux, 1988) by using a nonlinear transformation (Lacadie, Fulbright, Rajeevan, Constable, & Papademetris, 2008) to determine the corresponding Brodmann area (BA). These voxels were further selected for reconstruction of EEG-alpha sources in the time domain.

Time Course of EEG-alpha Sources Associated with WM Processes

Power time series were obtained for each selected voxel as the squared envelope of the signal estimated with the Hilbert transform. We applied the same hierarchical statistical procedure as described earlier to first evaluate power increases relative to baseline and next to determine which of these increases were modulated by information load and/or sample–test similarity. Likewise, regression analyses with RTs for each one of these conditions were also computed on an individual basis before determining whether the beta coefficients were different from zero. If significant, then paired t tests were used to determine the time windows where regression lines were significantly different. All statistical tests were applied to consecutive time windows of 40 msec within the different intervals of interest and corrected for multiple comparisons with the maximum statistic approach (1000 randomizations, $\alpha = .05$).

Localization of Cortico-cortical Alpha-phase Synchronization

Significant voxels resulting from source power statistics were used as regions of reference for computing cortico-cortical alpha-phase synchronization maps. Phase synchronization between voxel estimates was computed by using the phase lag index (PLI; Stam, Nolte, & Daffertshofer, 2007). This index measures the asymmetry of the phase difference distribution between two signals, meaning that their phase difference not only remains bound but also has a preferred orientation to one of the two halves of the unit circle. Each PLI value was obtained by averaging all trials for each time sample. Resulting PLI maps included the mean PLI from all time samples within the analysis window for each voxel. Because PLI values range from 0 (*lack of neural coupling*) to 1 (*perfect phase locking*), before applying the statistic they were z-transformed according to the equation $zPLI = n \times PLI^2$ (Fisher, 1993) that corrects for the number of trials (n).

Determining the Effect of Memory Load and Sample–Test Similarity on Alpha-phase Synchronization

The effect of WM load on alpha-phase synchronization was evaluated at the group level. First, individual zPLI maps were smoothed with a Gaussian kernel of 10 mm implemented in SPM5. Differences between LL and HL were only tested on those cortical regions showing significant zPLI increases when compared with the baseline in at least one of the two conditions. After baseline comparisons, we normalized the values from each condition dividing by the zPLI of the baseline. These contrasts were assessed by paired-sample t tests. To deal with the problem of multiple comparisons, we followed the same approach as described above for the source activation maps together with a cluster analysis.

PLI values were also computed in the time domain following a similar procedure as described for the PLI maps. To obtain meaningful values of alpha-phase synchronization, mean PLI values were obtained for each 500-msec averaging window (125 samples), in steps of 40 msec that includes at least four alpha cycles of 8 Hz. Then time series of zPLI values were compared with the zPLI value of the baseline period. To test whether modulations on alpha-phase synchronization had some physiological meaning, we used a bootstrap method (Lachaux, Rodriguez, Martinerie, & Varela, 1999). For each pair of source estimates, 1000 surrogate data were created by randomly

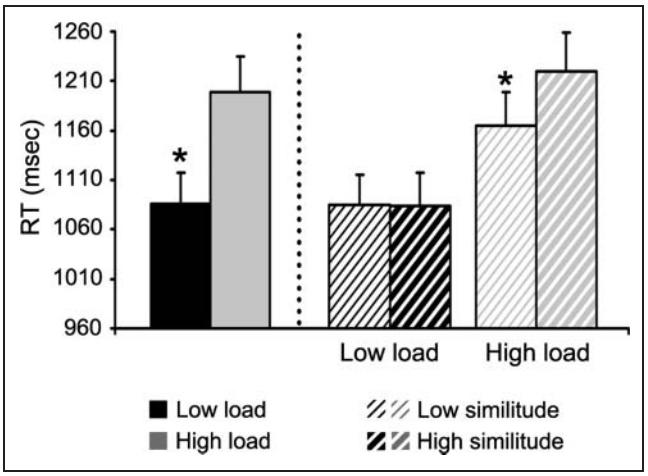

Figure 2. Effect of load and sample–test similarity on performance. Mean RTs for low and high memory load and for low and high sample–test similarity in each load condition. Error bars are standard errors of the mean. Asterisk indicates significant differences between conditions.

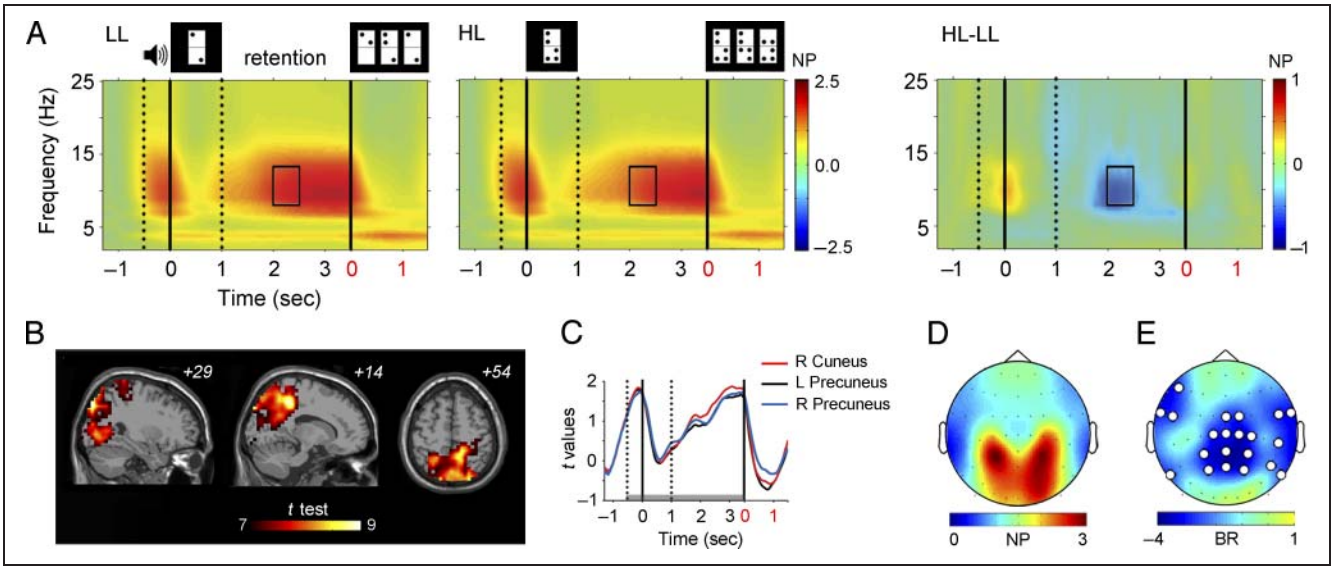

Figure 3. Time–frequency dynamics of alpha oscillations under different memory load conditions. (A) TFRs averaged over trials, electrodes, and participants for the low-load (LL) and high-load (HL) condition. TFR of the power difference (HL − LL) is shown in the plot on the right. The color-coded scale indicates modulations in oscillatory normalized power (NP) relative to baseline. Continuous vertical lines indicate the onset of the sample and test stimuli, whereas dotted vertical lines refer to the onset of the auditory tone and the retention period (sample stimulus offset). The black square represents the time–frequency window where source localization of alpha oscillations was estimated. Red numbers on the *x* axis indicate the time relative to the test stimulus onset. (B) Source localization of EEG-alpha oscillations. Activated regions are shown on the sagittal and axial views of Colin27 standard brain at $p < .001$ (cluster corrected). Peak voxels are listed in the text. (C) Time reconstruction of EEG-alpha sources for peak voxels in the right cuneus and bilateral precuneus. Waveforms represent the grand average of single-participant *t* tests of power time series relative to baseline in the two load conditions. The horizontal gray bar indicates the time interval of increased alpha power relative to baseline. Red numbers on the *x* axis indicate the time relative to the test stimulus onset. (D) Topographic distribution of normalized alpha power (NP) averaged across participants during the time–frequency window used for source localization. (E) Topographic statistical map obtained from the PLS analysis. Blue regions represent higher alpha power for LL than for HL conditions. White circles indicate electrodes where this effect was significant. BR = ratios of salience to bootstrap standard errors.

shuffling the trials from one of the source signals. We controlled that source activities belonging to the same original trial were never paired together. Surrogate data were then used to compute a distribution of 1000 PLI values for each source pair and time window. Values corresponding to the 95th quantile of the distribution were selected, yielding a threshold PLI time course for each source pair and participant. Original PLI time courses were contrasted to these threshold PLI time courses using Wilcoxon tests at the group level. Finally, we determined the effect of information load and/or sample–test similarity at the group level by applying the maximum statistic approach to correct for multiple comparisons across time (Nichols & Holmes, 2002).

Cross-correlations between EEG-alpha Sources in the Time Domain

Time series of anterior and posterior EEG-alpha sources showing significant phase synchronization within specific time intervals were submitted to cross-correlation analyses on a single-trial basis. We obtained a cross-correlogram for each single trial displaying correlation coefficients as a function of latency shift between the signals of the two EEG sources. The source signals were shifted by always one sample point (4 msec) in respect to each other. Finally, cross-correlograms were averaged over trials for each participant and condition (memory load and sample–test similarity), and latencies of maximal correlation coefficients were selected for subsequent statistical analyses at the group level. If pFC drives activity in posterior cortical regions, the highest correlation is expected to occur at a latency shift higher than 0. Consistency of latency shifts was evaluated across participants with one-sample *t* tests.

RESULTS

Behavioral Results

As expected, participants were slower in identifying the test stimulus ($p < 10^{-5}$) for the HL condition (RT_{HL} = 1198 msec, *SEM* = 35.8 msec) than for the LL condition (RT_{LL} = 1086 msec, *SEM* = 31.6 msec). Although the proportion of correct responses exceeded 90% in the two conditions, a significant decrease of correct responses was observed with increasing memory load ($p < .001$).

As expected from the two-factor model of WM function (Awh et al., 2007), the higher the number of spots in the domino tile, the lower the dissimilarity index ($r = -.35$,

$p < 10^{-6}$). In fact, participants were slower with increasing sample–test similarity ($p < .02$), but this effect was only evident in the HL condition ($p < .001$). For instance, when the tiles included four to five spots, RTs were 54 msec slower for trials with a low (mean = 1218.8 msec, *SEM* = 38.7 msec) than with a high dissimilarity index (mean = 1164.6 msec, *SEM* = 33.1 msec). These results are illustrated in Figure 2.

Cortical Dynamics of EEG-alpha Sources

Analyses applied on the total activity at the sensor level revealed a marked alpha increase in response to the warning tone ($p < 10^{-4}$; latent variable with singular value of 101.9, explaining ~100% of the covariance). This alpha increase began 100 msec after tone onset and ended 400 msec following sample stimulus onset. It was maximal over centro-parietal electrodes (Cp3 and CP4) and was neither affected by memory load (see TFRs included in Figure 3A) nor by sample–test similarity. In line with this topographic distribution, the main EEG-alpha sources were located in the bilateral parieto-occipital cortex (Figure 4A), particularly in the cuneus (BA 19; right MNI coordinates: 19 −90 39, $t = 9.2$, $p < .001$; left MNI coordinates: −11 −80 39, $t = 9.0$, $p < .001$) and precuneus (BA 7, 31; right MNI coordinates: 24 −45 39, $t = 9.7$, $p < .001$; left MNI coordinates: −21 −70 24, $t = 8.9$, $p < .001$).

Although the topographic distribution of alpha power in response to the warning tone (Figure 4C) was quite similar to the one observed during the retention period (Figure 3D), the time course of the EEG-alpha source located in pFC (Figure 4B) was quite different in the two intervals when analysis was restricted to non-phase-locked oscillations. Thus, alpha activity in the left superior frontal gyrus (BA 9; MNI coordinates: −6 60 24; $t = -6.6$; $p < .05$) was desynchronized with respect to the baseline from tone onset up to sample stimulus offset.

The retention period was characterized by alpha resynchronization (Figure 3A). This enhancement was significantly

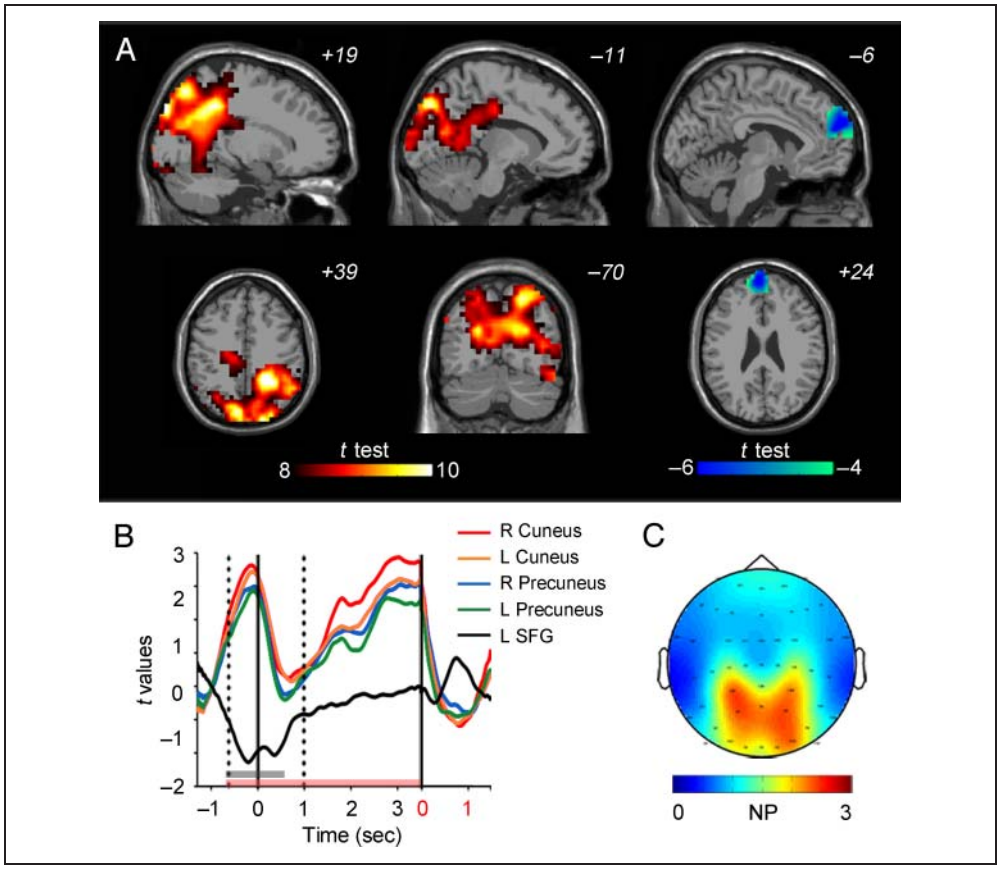

Figure 4. EEG-alpha sources and time course of alpha oscillations in response to the warning tone. (A) EEG-alpha sources within 500 msec after tone onset in the two load conditions. Activated regions on the Colin27 standard brain represent alpha power increases (red-to-yellow color; $p < .001$, cluster corrected) and alpha power decreases (green-to-blue color; $p < .05$, cluster corrected) observed in total and non-phase-locked activity, respectively. Peak voxels are listed in the text. (B) Time reconstruction of EEG-alpha sources for peak voxels in bilateral cuneus, bilateral precuneus, and left superior frontal gyrus (SFG). Waveforms represent the grand average of single-participant *t* tests of power time series relative to baseline in the two load conditions. Vertical lines refer to the same intervals described in the legend of Figure 3. Horizontal bars indicate statistically significant power increases (pink) or decreases (gray) relative to baseline. Red numbers on the *x* axis indicate the time relative to the test stimulus onset. (C) Topographic map of alpha power distribution during the auditory tone, averaged across participants. NP = normalized power relative to baseline.

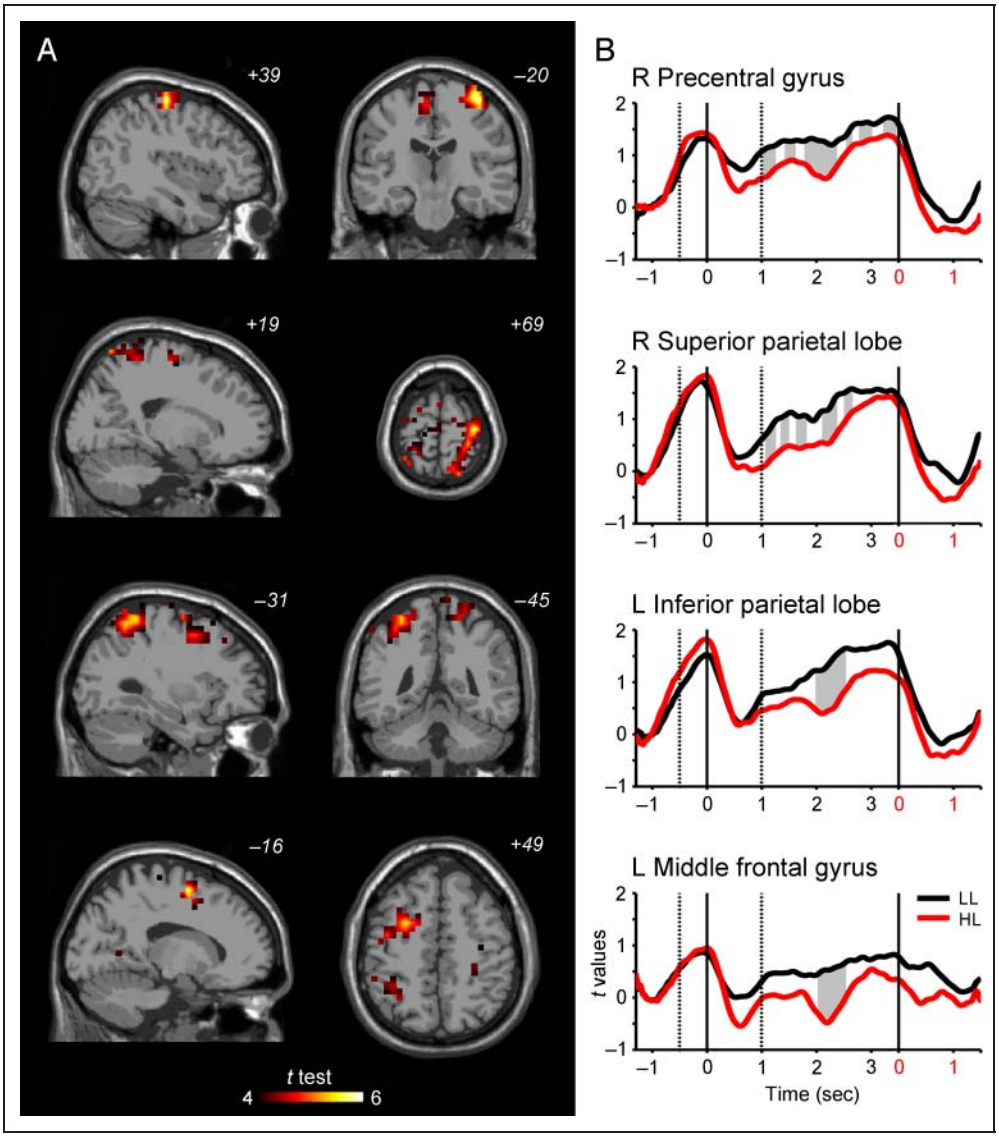

Figure 5. Source localization of load-dependent changes in alpha power and subsequent time reconstruction. (A) Statistical nonparametric maps obtained from the group-level analysis showing cortical regions that exhibited significant decreases of alpha power with memory load. Activated regions are shown on the orthogonal views of Colin27 standard brain at $p < .001$ (cluster corrected). Peak voxels are listed in Table 1. (B) Source waveforms showing significant load-related modulations in the time domain. Gray-shadowed vertical areas indicate significant differences between low-load (LL, black) and high-load (HL, red) conditions after correcting for multiple comparisons across time. Vertical lines refer to the same intervals described in the legend of Figure 3. Red numbers on the *x* axis indicate the time relative to the test stimulus onset.

less pronounced with increase in memory load from around 2000 to 2500 msec (Figure 3A, right) as revealed by the PLS analysis ($p < .013$; latent variable with singular value of 32.74, explaining ~100% of the covariance). This effect of WM load on alpha power was mainly evident over centro-parietal regions, although sensors in left anterior and right temporal also reached statistical significance (Figure 3E).

Table 1. Peak Voxels of BA Showing Significant Differences in Alpha Activity with Memory Load (Whole-brain Corrected)

Brain Region	*BA*	*x*	*y*	*z*	*t*	*p*
LL > HL						
L middle frontal gyrus	6	−16	0	59	5.59	.010
R precentral gyrus	4	39	−20	64	6.02	.009
R superior parietal lobe	7	19	−65	69	5.01	.033
L inferior parietal lobe	40	−31	−45	64	5.53	.013

Voxel coordinates are in MNI space. L = left; R = right.

Consistent with the topographic distribution observed at the level of sensors within the above-mentioned time interval (Figure 3D), the EEG sources mainly responsible for alpha enhancement were located in the parieto-occipital cortex (Figure 3B), with maxima (voxel level) observed in the right cuneus (BA 19; MNI coordinates: 29 −85 44; $t = 9.4$; $p < .001$) and bilateral precuneus/posterior cingulate (BA 7; right MNI coordinates: 14 −40 44; $t = 9.1$; $p < .001$; left MNI coordinates: −16 −80 54; $t = 8.6$; $p < .001$). This alpha increase reached its maximum amplitude at the end of the retention interval and returned to baseline after presentation of the test stimulus as can be seen on the *t* statistic obtained from reconstructed source time courses (Figure 3C).

The contrasts for evaluating the influence of memory load at the level of sources revealed a higher increase of alpha power for LL than for HL condition ($p < .05$) in the PPC and frontal lobe (Figure 5A). Table 1 contains

Table 2. Peak Voxels of Clusters Showing Significant Differences in Alpha PLI for Different Contrasts (Cluster-corrected, $p < .05$)

Brain Region	*BA*	*x*	*y*	*z*	*t*	*Number of Voxels*	*p*
PLI between L middle frontal gyrus (retention < baseline)	6						
and L superior frontal gyrus	8	−16	40	44	−4.35	645	.031
and R superior frontal gyrus	8	14	60	34	−4.27	645	.031
PLI between R precentral gyrus (retention > baseline)	4						
and L anterior cingulate gyrus	32	−21	10	34	6.04	626	.032
PLI between L inferior parietal lobe (retention > baseline)	40						
and L anterior cingulate gyrus	24	−1	−5	34	5.07	1188	.014
and L inferior parietal lobe	40	−41	−45	49	4.29	1188	.014
and L middle frontal gyrus	46	−46	40	14	3.98	1188	.014
PLI between L precuneus (retention > baseline)	7						
and R paracentral lobule	5	24	−35	49	5.89	1277	.008
PLI between L inferior parietal lobe (LL > HL)	40						
and L anterior cingulate gyrus	32	−16	15	29	4.06	251	.004
and L middle frontal gyrus	6	−41	20	54	3.73	251	.004

Voxel coordinates are in MNI space. L = left; R = right.

voxel coordinates showing the maximum difference for each significant BA. Figure 5B shows the *t* statistic for each significant EEG-alpha source and the time intervals where the amplitude was significantly modulated by memory load (shadowed vertical area). The time course analysis revealed significant load effects in the right precentral gyrus (BA 4, 1000–3400 msec, $t > 2.9$, $p < .05$), right superior parietal lobe (BA 7, 1040–2600 msec, $t > 3.1$ $p < .05$), left inferior parietal lobe (BA 40, 1920–2480 msec, $t > 3.1$, $p < .05$), and left middle frontal gyrus (BA 6, 2000–2480 msec, $t > 3.4$, $p < .02$). None of these signals showed significant correlations with behavior.

No effect of sample–test similarity could be observed in any time interval at alpha frequency, not even when analyses were performed in each load condition separately. At the sensor level, results during retrieval revealed a significant effect of sample–test similarity over the linear regressions between upper alpha (10–13 Hz) power and behavior ($p < .05$) that was particularly evident in Pz. However, alpha activity in this time–frequency range did not differ from baseline, which made impossible source estimation. When the analysis was applied on the time series reconstructed from sources estimated during retention, correlations were not significant in either condition.

Cortico-cortical Patterns of Alpha-phase Synchronization

Alpha activity in the left inferior parietal lobe and left precuneus showed enhanced phase synchronization with alpha oscillations in regions of the frontal lobe during retention (see Table 2). But only the functional connectivity with the left inferior parietal lobe was modulated by information load. Specifically, we found that interregional phase synchrony with the left inferior parietal lobe in the HL condition was significantly lower than in the LL condition (Figure 6A). Analyses in the time domain revealed that these differences were evident between 1060 and 3280 msec ($t > 2.76$, $p < .05$) for functional connections with the left anterior cingulate gyrus (BA 32) and between 1420 and 3480 msec ($t > 2.73$, $p < .05$) for functional connections with the left middle frontal gyrus (BA 6). Analysis of consistency of the latency shifts between these EEG-alpha sources revealed a significant delay of 15 msec ($p < .001$) from the left middle frontal gyrus to the left inferior parietal lobe in the LL and HL conditions (Figure 6C). Interestingly, PLI analyses also yielded a significant reduction of alpha-phase synchrony during retention relative to baseline between regions located in the frontal lobe (Table 2), particularly between the left middle frontal gyrus (BA 6) and bilateral superior frontal gyrus (BA 8), but no consistent latency shifts were found in either direction.

DISCUSSION

The major results of this study are that load-dependent and load-independent EEG-alpha oscillatory dynamics coexist in different cortical regions during WM retention. In particular, we found load-independent increases of alpha

power in task-irrelevant regions of the visual pathway and load-dependent decreases in regions of the WM network including the prefrontal and PPCs. The former results support the functional inhibitory role of alpha oscillations, whereas the latter likely reflect release of task-relevant areas from inhibition with load increase. This study also showed interregional functional alpha coupling between anterior and posterior cortical regions of the WM network under LL conditions (but not when memory load was increased) as well as a significant latency shift from pFC to the PPC, which is in line with the role of pFC in inhibitory control of higher visual areas.

Alpha Dynamics in Task-irrelevant Regions during WM Retention

Participants showed alpha power increases in posterior regions during the retention interval that not only were independent of information load but also of resolution of representations. Consistent with previous magnetoencephalographic studies, the highest amplitude of this EEG oscillatory activity was located quite near the parieto-occipital sulcus (Vanni et al., 1997). The equivalent region in monkeys has been suggested to participate in visual space encoding (Galletti, Battaglini, & Fattori, 1991, 1995), which would support the inhibitory role of alpha activity in this region. In line with this interpretation, Jokisch and Jensen (2007) reported increased alpha power around the parieto-occipital sulcus during retention of face identity but not during retention of face orientation. Alpha increase was thought to protect the relevant neural representation of the face identity from task-irrelevant information about orientation. The physiological function of the inhibitory process reflected by alpha oscillations over task-irrelevant regions would be to direct the information flow to task-relevant cortical structures (Klimesch et al., 2007, 2011; Jensen & Mazaheri, 2010). The progressive increase of alpha power over the retention period may then reflect gradual attenuation of information transfer and disengagement of parieto-occipital regions during WM maintenance, which is further supported by fMRI studies showing negative correlations with the BOLD

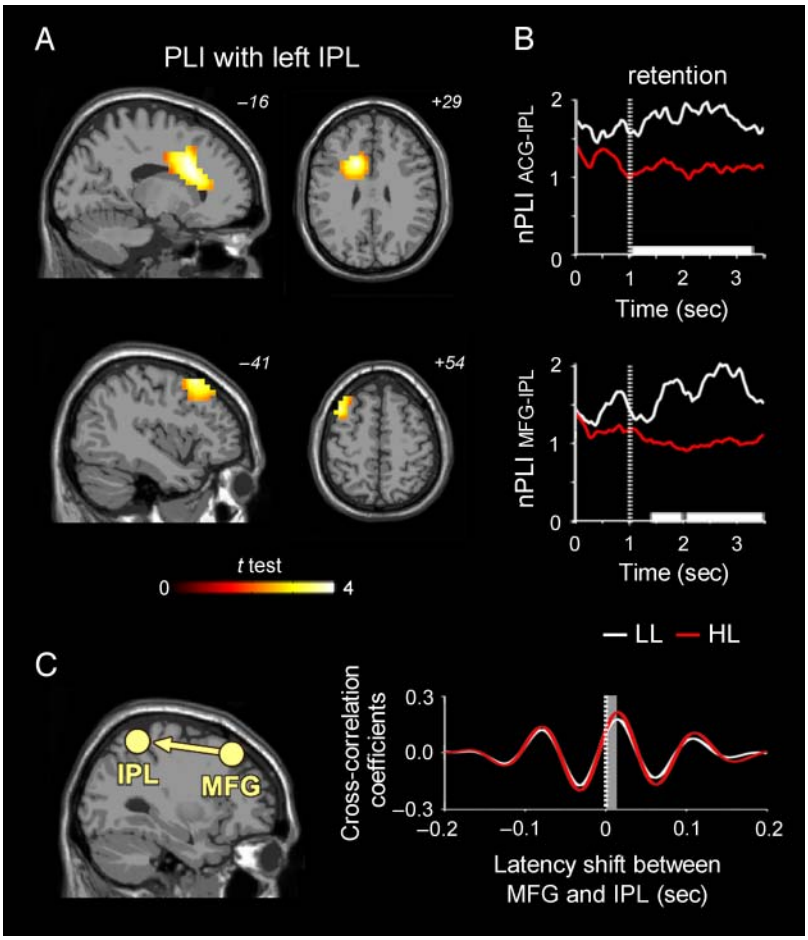

Figure 6. Load-dependent decreases of alpha-phase synchrony between frontal and parietal regions. (A) Statistical nonparametric maps obtained from the group-level analysis showing cortical regions that exhibited load-induced decrease of interregional phase synchrony with the left inferior parietal lobe (IPL). Results are shown on the sagittal and axial views of Colin27 standard brain at $p < .001$ (cluster corrected). Peak voxels referring to the left anterior cingulate gyrus (ACG) and left middle frontal gyrus (MFG) are listed in Table 2. (B) Time course of the normalized PLI values (nPLI) relative to baseline for the low-load (LL, white) and high-load (HL, red) condition. White horizontal bars over the *x* axis indicate the time windows where the two conditions were statistically different. The dotted vertical line indicates the onset of the retention period. (C) Top–down interaction in the alpha band during the retention period. Representation of MFG and IPL alpha sources (yellow circles) on the Colin27 standard brain, indicating that the prefrontal source is leading the parietal source, as inferred from the cross-correlation analysis. The plot on the right shows the cross-correlation coefficients, averaged across trials and participants for each load condition, as a function of the latency shift between MFG and IPL. Note that the highest correlation between the two sources shows a positive lag of 15 msec (indicated by the gray-shadowed area) in the two load conditions, which agrees with the expected delay in the fronto-posterior neural transmission.

signal (Michels et al., 2010; Meltzer et al., 2008). Consistent with our results, neither alpha activity nor the BOLD signal was modulated by memory load in the regions surrounding the parieto-occipital sulcus.

The load-independent increase of posterior alpha power was accompanied by load-independent increases of alpha-phase synchrony between two medial portions of the superior parietal cortex, left precuneus, and right paracentral lobule (BA 5). Functional connectivity analyses of the precuneus in humans and macaque monkeys have revealed that the anterior portion of the precuneus is functionally connected to the paracentral lobule and motor cortex (Margulies et al., 2009). Consequently, this enhanced alpha-phase synchronization during WM retention might be another neural signature of an inhibitory process that acts to diminish the flow of sensorimotor information.

Alpha Dynamics in Task-relevant Regions during WM Retention

The alpha power increase during the retention interval was of smaller magnitude under HL conditions as compared with LL conditions over regions of the PPC, premotor cortex, and pFC, all of them known to be part of the frontoparietal network involved in WM processes (e.g., Cabeza & Nyberg, 2000).

Many studies have supported the hypothesis that the right parietal lobe in general and the intraparietal sulcus in particular play a critical role in the active maintenance of spatial information in WM (e.g., Berryhill & Olson, 2008). A recent fMRI study showed that bilateral activation of intraparietal sulci that is predictive of individual WM capacity (Todd & Marois, 2004) correlated with the amount of retained spatial information (Harrison, Jolicoeur, & Marois, 2010). In line with the above-mentioned results, the smaller increase of alpha power in the left inferior and right superior parietal lobe with load increase may reflect a partial release from an inhibitory action on the parietal dorsal stream. In agreement with these findings, Gevins et al. (1997) reported attenuated alpha power over parieto-central and occipito-parietal sites with an increasing load in a task that manipulated the spatial location of letters. Contrary to our results, there is also evidence of alpha power enhancements with increasing load by adding spatial elements (i.e., Palva et al., 2011; Grimault et al., 2009), but stimulus identification was based on color information, an attribute that is primarily processed in the ventral stream (Zeki, 1990).

The decrease of alpha power with memory load was especially evident in the frontal lobe, particularly in the left middle frontal gyrus (BA 6). This result replicates those of previous EEG studies (Stipacek et al., 2003; Krause et al., 2000). The anterior load-dependent alpha response has been proposed as a neural correlate of the central executive component (Stipacek et al., 2003). This interpretation is in agreement with models that attribute storage functions or representations to posterior cortical areas and executive operations to pFC (D'Esposito, Postle, & Rypma, 2000; Petrides, 2000; Smith & Jonides, 1999). Interestingly, the opposite result (load-dependent alpha event-related synchronization) has been interpreted in the same terms. Indeed, all previous studies showing alpha power increases over frontal regions with memory load saw this enhancement as a top–down control signal (Michels et al., 2010; Grimault et al., 2009; Scheeringa et al., 2009; Leiberg et al., 2006; Sauseng, Klimesch, Doppelmayr, et al., 2005). Alternatively, the distinct load modulations of alpha power might indicate that different regions within pFC are recruited depending on the operations required in each WM task.

In the present study, load-dependent changes of alpha oscillations in the left middle frontal gyrus may be indicative of top–down inhibition. This region is regarded as part of the dorsolateral pFC. Although its right side seems to play a strategic planning role, the left one has been proposed to be specifically involved in the cognitive control processes required to provide top–down support (Newman, Just, & Carpenter, 2002). According to the large-scale integration framework (von Stein & Sarnthein, 2000; see also Palva & Palva, 2011), alpha-phase interactions may underlie top–down modulations of local oscillatory activity in parietal regions driven by pFC. In line with this interpretation, our results revealed a load-induced decrease of alpha-phase synchrony between the left middle frontal gyrus and the left inferior parietal lobe. In addition, cross-correlograms for trials with low information load showed a significant latency shift of 15 msec from the former to the latter, which might suggest that information flow was predominant in that direction. This phase lag lies within a time range that is consistent with neuronal transmission speed and is in agreement with other similar reports (Sauseng, Feldheim, Freunberger, & Hummel, 2011; Schack, Weiss, & Rappelsberger, 2003). In particular, Sauseng et al. (2011) found that the inhibitory mechanism imposed by increased alpha activity ipsilateral to the attended location was partially controlled by the right FEFs. Therefore, it is likely that the inhibitory role of alpha oscillations in the parietal lobe and the load-induced release from such inhibition are under prefrontal control. In spite of these evidences, we should be cautious when interpreting directionality derived from cross-correlation analyses because phase-lag is not a reliable measure of causal relations between sources. To test the direction of information flow between distant neural assemblies, other mathematical approaches based on Granger causality or information theory are more suitable (Pereda et al., 2005). However, important assumptions as signal stationarity and the large amount of data necessary for applying these causal measures have limited their applicability in our study.

Alternatively, load modulations of alpha power and interregional alpha-phase synchronization could reflect maintenance of more visual details when dominoes included a higher number of spots, as would be predicted from the

two-factor model of WM function (Awh et al., 2007). This model states that the number of representations that can be maintained in WM and the resolution of such representations represent two independent components of WM capacity. Accordingly, we found that similarity between the test and distractor domino tiles during retrieval was a determinant factor of performance for dominoes with higher information load. On the basis of fMRI results (Xu & Chun, 2006), it has been suggested that activity within the inferior intraparietal sulcus may determine how many representations can be stored, whereas activity in the superior intraparietal sulcus and lateral occipital regions may determine the resolution of those representations (Anderson et al., 2011; Awh et al., 2007). In line with this prediction, alpha oscillations in the inferior parietal lobe should be selectively affected by information load whereas alpha in the superior parietal lobe should be further affected by sample–test similarity (at least in the HL condition). Our results did not confirm this hypothesis because neither alpha power nor interregional alpha-phase synchrony was modulated by sample–test similarity in any time interval. A possible explanation for this result is that the effect of resolution is not indexed by alpha oscillations. Additionally, it is feasible that the experimental design was not optimal for testing this hypothesis. It is important to note that load variations in most previous studies were related to increasing the number of items currently held in WM, which required maintenance of more precise representations during the retention period to support performance in memory tasks with complex stimuli. On the contrary, our participants were always asked to maintain one domino piece, so comparison errors could only happen during retrieval, when the sample stimulus had to be identified among three domino tiles. As these tiles are present until participants give their responses, no additional internal representations are required, which would account for the lack of effect in this time interval.

Alpha Dynamics during the Prestimulus and Encoding Interval

The role of alpha oscillations has been related to the state of brain activation and to the timing of information processing regardless of whether they occur in the pre- or poststimulus interval (Klimesch et al., 2007). In the present study, alpha increase was observed in response to the initial tone as well as during WM retention. Although these responses were apparently similar, only the former showed a component that was phase-locked to the stimulus and consequently they reflect different aspects of inhibition. In the retention interval, the long-lasting alpha power increase is thought to maintain low excitability in parieto-occipital regions of the cortex, which likely facilitates information processing in other task-relevant regions (Mathewson et al., 2011; Jensen & Mazaheri, 2010; Klimesch et al., 2007). However, the event-related alpha increase elicited by the warning tone in the same cortical regions might reflect enhanced processing in these regions at a particular phase of alpha oscillations. It has been suggested that alpha oscillations only reflect periods of low and high neural excitability when the power is high (Mathewson et al., 2011). In this study, the warning tone always alerted of the arrival of a visual stimulus 500 msec later, which made the upcoming stimulus highly predictable in time. We propose that the increased alpha power in response to the tone reflects this high level of predictability.

In addition, the early increase of alpha power was accompanied by a non-phase-locked alpha desynchronization in the superior frontal gyrus, which is indicative of active involvement of the underlying neuronal tissue. Evidence suggests that this response is associated with increased attention directed externally to the environment (Rajagovindan & Ding, 2010; Sauseng, Klimesch, Stadler, et al., 2005; Worden et al., 2000). Therefore, alpha synchronization and alpha desynchronization in the prestimulus interval might result from two different mechanisms aimed at facilitating processing of the domino tile in the visual cortex.

Conclusions

Manipulations of information load produced decreases in the amplitude and interregional coupling of alpha oscillations during WM retention in different cortical regions of the WM network. This phenomenon was further accompanied by load-independent increases of local and long-range synchronization at alpha frequency in parieto-occipital regions. These findings suggest that different neural mechanisms indexed by alpha oscillatory activity can coexist. Particularly, increase of memory load produced three types of changes in the alpha band: decrease of local synchronization in regions of the PPC, increase of local desynchronization in pFC, and decrease of long-range interregional synchronization between pFC and PPC with a significant latency shift from the left middle frontal gyrus to the left inferior parietal lobe. These results are consistent with the view of a top–down, inhibitory control exerted by alpha oscillations over the timing of cortical processing (Klimesch et al., 2007). However, it is important to note that none of these alpha modulations correlated with performance, likely because RTs in this study were mainly determined by comparison errors during retrieval rather than by changes in memory load. Unfortunately, the experimental design of this study did not allow us to determine whether changes in the amplitude and phase of alpha oscillations can distinguish between the two components of WM function proposed by Awh et al. (2007). Future research is needed to shed light in that particular direction.

Acknowledgments

This study was supported by research grants from the Spanish Ministry of Science and Innovation MICINN (SEF2007-67964-C02-02, SAF2011-25463, BES-2008-005929, PSI2010-22224-C03-03,

and PSI2011-24922), the Regional Ministry of Innovation, Science and Enterprise of the Junta de Andalucia (P09-CTS-4604), the Galician Consellería de Innovación e Industria (PGIDIT07P-XIB211018PR), and the Educación e Ordenación Universitaria (Redes Novas. Expte. 2010/56, FEDER funds).

Reprint requests should be sent to Mercedes Atienza, Laboratory of Functional Neuroscience, Spanish Network of Excellence for Research on Neurodegenerative Disease. (CIBERNED) University Pablo de Olavide, Carretera de Utrera Km 1, 41013 Seville, Spain, or via e-mail: matirui@upo.es.

REFERENCES

Anderson, D. E., Vogel, E. K., & Awh, E. (2011). Precision in visual working memory reaches a stable plateau when individual item limits are exceeded. *The Journal of Neuroscience, 31,* 1128–1138.

Awh, E., Barton, B., & Vogel, E. K. (2007). Visual working memory represents a fixed number of items regardless of complexity. *Psychological Science, 18,* 622–628.

Baddeley, A. (1998). The central executive: A concept and some misconceptions. *Journal of the International Neuropsychological Society: JINS, 4,* 523–526.

Baddeley, A. (2002). The episodic buffer: A new component of working memory? *Trends in Cognitive Sciences, 4,* 417–423.

Berryhill, M. E., & Olson, I. R. (2008). The right parietal lobe is critical for visual working memory. *Neuropsychologia, 46,* 1767–1774.

Bollimunta, A., Chen, Y., Schroeder, C. E., & Ding, M. (2008). Neuronal mechanisms of cortical alpha oscillations in awake-behaving macaques. *Journal of Neuroscience, 28,* 9976–9988.

Busch, N. A., & Herrmann, C. S. (2003). Object-load and feature-load modulate EEG in a short-term memory task. *NeuroReport, 14,* 1721–1724.

Cabeza, R., & Nyberg, L. (2000). Neural bases of learning and memory: Functional neuroimaging evidence. *Current Opinion in Neurology, 13,* 415–421.

Cooper, N. R., Croft, R. J., Dominey, S. J., Burgess, A. P., & Gruzelier, J. H. (2003). Paradox lost? Exploring the role of alpha oscillations during externally vs. internally directed attention and the implications for idling and inhibition hypotheses. *International Journal of Psychophysiology, 47,* 65–74.

Dalal, S. S., Sekihara, K., & Nagarajan, S. S. (2006). Modified beamformers for coherent source region suppression. *IEEE Transactions on Bio-medical Engineering, 53,* 1357–1363.

D'Esposito, M., Postle, B. R., & Rypma, B. (2000). Prefrontal cortical contributions to working memory: Evidence from event-related fMRI studies. *Experimental Brain Research, 133,* 3–11.

Diwakar, M., Huang, M. X., Srinivasan, R., Harrington, D. L., Robb, A., Angeles, A., et al. (2011). Dual-core Beamformer for obtaining highly correlated neuronal networks in MEG. *Neuroimage, 54,* 253–263.

Fisher, N. I. (1993). *Statistical analysis of circular data*. Cambridge, U.K.: Cambridge University Press.

Fletcher, P. C., Frith, C. D., Baker, S. C., Shallice, T., Frackowiak, R. S. J., & Dolan, R. J. (1995). The mind's eye-precuneus activation in memory related imagery. *Neuroimage, 2,* 195–200.

Galletti, C., Battaglini, P. P., & Fattori, C. (1991). Functional properties of neurons in the anterior bank of the parieto-occipital sulcus of the macaque monkey. *European Journal of Neuroscience, 3,* 452–461.

Galletti, C., Battaglini, P. P., & Fattori, P. (1995). Eye position influence on the parieto-occipital area PO (V6) of the macaque monkey. *European Journal of Neuroscience, 7,* 2486–2501.

Gevins, A., Smith, M. E., McEvoy, L., & Yu, D. (1997). High-resolution EEG mapping of cortical activation related to working memory: Effects of task difficulty, type of processing, and practice. *Cerebral Cortex, 7,* 374–385.

Grimault, S., Robitaille, N., Grova, C., Lina, J. M., Dubarry, A. S., & Jolicoeur, P. (2009). Oscillatory activity in parietal and dorsolateral prefrontal cortex during retention in visual short-term memory: Additive effects of spatial attention and memory load. *Human Brain Mapping, 30,* 3378–3392.

Gundel, A., & Wilson, G. F. (1992). Topographical changes in the ongoing EEG related to the difficulty of mental tasks. *Brain Topography, 5,* 17–25.

Haenschel, C., Bittner, R. A., Waltz, J., Haertling, F., Wibral, M., Singer, W., et al. (2009). Cortical oscillatory activity is critical for working memory as revealed by deficits in early-onset schizophrenia. *Journal of Neuroscience, 29,* 9481–9489.

Harrison, A., Jolicoeur, P., & Marois, R. (2010). "What" and "where" in the IPS: And fMRI study of object identity and location in visual short-term memory. *Cerebral Cortex, 20,* 2478–2485.

Jensen, O., Gelfand, J., Kounios, J., & Lisman, J. E. (2002). Oscillations in the alpha band (9–12 Hz) increase with memory load during retention in a short-term memory task. *Cerebral Cortex, 12,* 877–882.

Jensen, O., & Mazaheri, A. (2010). Shaping functional architecture by oscillatory alpha activity: Gating by inhibition. *Frontiers in Human Neuroscience, 4,* 186.

Jokisch, D., & Jensen, O. (2007). Modulation of gamma and alpha activity during a working memory task engaging the dorsal or ventral stream. *Journal of Neuroscience, 27,* 3244–3251.

Kelly, S. P., Lalor, E. C., Reilly, R. B., & Foxe, J. J. (2006). Increases in alpha oscillatory power reflect an active retinotopic mechanism for distracter suppression during sustained visuo-spatial attention. *Journal of Neurophysiology, 95,* 3844–3851.

Klimesch, W., Fellinger, R., & Freunberger, R. (2011). Alpha oscillations and early stages of visual encoding. *Frontiers in Psychology, 2,* 118.

Klimesch, W., Sauseng, P., & Hanslmayr, S. (2007). EEG alpha oscillations: The inhibition-timing hypothesis. *Brain Research Reviews, 53,* 63–88.

Krause, C. M., Sillanmäki, L., Koivisto, M., Saarela, C., Häggqvist, A., Laine, M., et al. (2000). The effects of memory load on event-related EEG desynchronization and synchronization. *Clinical Neurophysiology, 111,* 2071–2078.

Lacadie, C. M., Fulbright, R. K., Rajeevan, N., Constable, R. T., & Papademetris, X. (2008). More accurate Talairach coordinates for neuroimaging using non-linear registration. *Neuroimage, 42,* 717–725.

Lachaux, J. P., Rodriguez, E., Martinerie, J., & Varela, F. J. (1999). Measuring phase synchrony in brain signals. *Human Brain Mapping, 8,* 194–208.

Leiberg, S., Lutzenberger, W., & Kaiser, J. (2006). Effects of memory load on cortical oscillatory activity during auditory pattern working memory. *Brain Research, 1120,* 131–140.

Margulies, D. S., Vincent, J. L., Kelly, C., Lohmann, G., Uddin, L. Q., Biswal, B. B., et al. (2009). Precuneus shares intrinsic functional architecture in humans and monkeys.

Proceedings of the National Academy of Sciences, U.S.A., 106, 20069–20074.
Mathewson, K. E., Lleras, A., Beck, D. M., Fabiani, M., Ro, T., & Gratton, G. (2011). Pulsed out of awareness: EEG alpha oscillations represent a pulsed-inhibition of ongoing cortical processing. *Frontiers in Psychology, 2,* 99.
Meltzer, J. A., Zaveri, H. P., Goncharova, I. I., Distasio, M. M., Papademetris, X., Spencer, S. S., et al. (2008). Effects of working memory load on oscillatory power in human intracranial EEG. *Cerebral Cortex, 18,* 1843–1855.
Michels, L., Bucher, K., Lüchinger, R., Klaver, P., Martin, E., Jeanmonod, D., et al. (2010). Simultaneous EEG-fMRI during a working memory task: Modulations in low and high frequency bands. *PloS One, 5,* e10298.
Michels, L., Moazami-Goudarzi, M., Jeanmonod, D., & Sarnthein, J. (2008). EEG alpha distinguishes between cuneal and precuneal activation in working memory. *Neuroimage, 40,* 1296–1310.
Miller, E. K., Erickson, C. A., & Desimone, R. (1996). Neural mechanisms of visual working memory in prefrontal cortex of the macaque. *Journal of Neuroscience, 16,* 5154–5167.
Mo, J., Schroeder, C. E., & Ding, M. (2011). Attentional modulation of alpha oscillations in macaque inferotemporal cortex. *Journal of Neuroscience, 31,* 878–882.
Moore, T., & Armstrong, K. M. (2003). Selective gating of visual signals by microstimulation of frontal cortex. *Nature, 421,* 370–373.
Newman, S. D., Just, M. A., & Carpenter, P. A. (2002). The synchronization of the human cortical working memory network. *Neuroimage, 5,* 810–822.
Nichols, T. E., & Holmes, A. P. (2002). Nonparametric permutation tests for functional neuroimaging: A primer with examples. *Human Brain Mapping, 15,* 1–25.
Nunez, P. L., Srinivasan, R., Westdorp, A. F., Wijesinghe, R. S., Tucker, D. M., Silberstein, R. B., et al. (1997). EEG coherency. I. Statistics, reference electrode, volume conduction, Laplacians, cortical imaging, and interpretation at multiple scales. *Electroencephalography and Clinical Neurophysiology, 103,* 499–515.
Oldfield, R. C. (1971). The assessment and analysis of handedness: The Edinburgh inventory. *Neuropsychologia, 9,* 97–113.
Oostenveld, R., Fries, P., Maris, E., & Schoffelen, J. M. (2011). FieldTrip: Open source software for advanced analysis of MEG, EEG, and invasive electrophysiological data. *Computational Intelligence and Neuroscience, 2011,* 156869.
Oostenveld, R., Praamstra, P., Stegeman, D. F., & van Oosterom, A. (2001). Overlap of attention and movement-related activity in lateralized event-related brain potentials. *Clinical Neurophysiology: Official Journal of the International Federation of Clinical Neurophysiology, 112,* 477–484.
Palva, J. M., Monto, S., Kulashekhar, S., & Palva, S. (2010). Neuronal synchrony reveals working memory networks and predicts individual memory capacity. *Proceedings of the National Academy of Sciences, U.S.A., 107,* 7580–7585.
Palva, S., Kulashekhar, S., Hämäläinen, M., & Palva, J. M. (2011). Localization of cortical phase and amplitude dynamics during visual working memory encoding and retention. *Journal of Neuroscience, 31,* 5013–5025.
Palva, S., & Palva, J. M. (2007). New vistas for alpha-frequency band oscillations. *Trends in Neuroscience, 30,* 150–158.
Palva, S., & Palva, J. M. (2011). Functional roles of alpha-band phase synchronization in local and large-scale cortical networks. *Frontiers in Psychology, 2,* 204.
Percival, D. B., & Walden, A. T. (1993). *Spectral analysis for physical applications: Multitaper and conventional univariate techniques*. Cambridge, U.K.: Cambridge University Press.
Pereda, E., Quian Quiroga, R., & Bhattacharya, J. (2005). Nonlinear multivariate analysis of neurophysiological signals. *Progress in Neurobiology, 77,* 1–37.
Petrides, M. (2000). The role of the mid-dorsolateral prefrontal cortex in working memory. *Experimental Brain Research, 133,* 44–54.
Rajagovindan, R., & Ding, M. (2010). From prestimulus alpha oscillation to visual-evoked response: An inverted-U function and its attentional modulation. *Journal of Cognitive Neuroscience, 23,* 1379–1394.
Roland, P. E., Gulyás, B., Seitz, R. J., Bohm, C., & Stone-Elander, S. (1990). Functional anatomy of storage, recall and recognition of a visual pattern in man. *NeuroReport, 1,* 53–56.
Sauseng, P., Feldheim, J. F., Freunberger, R., & Hummel, F. C. (2011). Right prefrontal TMS disrupts interregional anticipatory EEG alpha activity during shifting of visuospatial attention. *Frontiers in Psychology, 2,* 241.
Sauseng, P., Klimesch, W., Doppelmayr, M., Pecherstorfer, T., Freunberger, R., & Hanslmayr, S. (2005). EEG alpha synchronization and functional coupling during top–down processing in a working memory task. *Human Brain Mapping, 26,* 148–155.
Sauseng, P., Klimesch, W., Schabus, M., & Doppelmayr, M. (2005). Frontoparietal EEG coherence in theta and upper alpha reflect central executive functions of working memory. *International Journal of Psychophysiology, 57,* 97–103.
Sauseng, P., Klimesch, W., Stadler, W., Schabus, M., Doppelmayr, M., Hanslmayr, S., et al. (2005). A shift of visual spatial attention is selectively associated with human EEG alpha activity. *European Journal of Neuroscience, 22,* 2917–2926.
Schack, B., & Klimesch, W. (2002). Frequency characteristics of evoked and oscillatory electroencephalic activity in a human memory-scanning task. *Neuroscience Letters, 331,* 107–110.
Schack, B., Weiss, S., & Rappelsberger, P. (2003). Cerebral information transfer during word processing: Where and when does it occur and how fast is it? *Human Brain Mapping, 19,* 18–36.
Scheeringa, R., Petersson, K. M., Oostenveld, R., Norris, D. G., Hagoort, P., & Bastiaansen, M. C. (2009). Trial-by-trial coupling between EEG and BOLD identifies networks related to alpha and theta EEG power increases during working memory maintenance. *Neuroimage, 44,* 1224–1238.
Singer, W. (2009). Distributed processing and temporal codes in neuronal networks. *Cognitive Neurodynamics, 3,* 189–196.
Smith, E. E., & Jonides, J. (1999). Storage and executive processes in the frontal lobes. *Science, 283,* 1657–1661.
Stam, C. J., Nolte, G., & Daffertshofer, A. (2007). Phase lag index: Assessment of functional connectivity from multi channel EEG and MEG with diminished bias from common sources. *Human Brain Mapping, 28,* 1178–1193.
Stipacek, A., Grabner, R. H., Neuper, C., Fink, A., & Neubauer, A. C. (2003). Sensitivity of human EEG alpha band desynchronization to different working memory components and increasing levels of memory load. *Neuroscience Letters, 353,* 193–196.
Talairach, J., & Tournoux, P. (1988). *Co-planar stereotaxic atlas of the human brain*. New York: Thieme.
Thut, G., Nietzel, A., Brandt, S. A., & Pascual-Leone, A. (2006). Alpha-band electroencephalographic activity over occipital cortex indexes visuospatial attention bias and predicts visual target detection. *Journal of Neuroscience, 26,* 9494–9502.
Todd, J. J., & Marois, R. (2004). Capacity limit of visual short-term memory in human posterior parietal cortex. *Nature, 428,* 751–754.

Tuladhar, A. M., ter Huurne, N., Schoffelen, J. M., Maris, E., Oostenveld, R., & Jensen, O. (2007). Parieto-occipital sources account for the increase in alpha activity with working memory load. *Human Brain Mapping, 28,* 785–792.

Vanni, S., Revonsuo, A., & Hari, R. (1997). Modulation of the parieto-occipital rhythm during object detection. *Journal of Neuroscience, 17,* 7141–7147.

von Stein, A., & Sarnthein, J. (2000). Different frequencies for different scales of cortical integration: From local gamma to long range alpha/theta synchronization. *International Journal of Psychophysiology, 38,* 301–313.

Womelsdorf, T., & Fries, P. (2007). The role of neuronal synchronization in selective attention. *Current Opinion in Neurobiology, 17,* 154–160.

Worden, M. S., Foxe, J. J., Wang, N., & Simpson, G. V. (2000). Anticipatory biasing of visuospatial attention indexed by retinotopically specific-band electroencephalography increases over occipital cortex. *Journal of Neuroscience, 20,* 1–6.

Xu, Y., & Chun, M. M. (2006). Dissociable neural mechanisms supporting visual short-term memory for objects. *Nature, 440,* 91–95.

Yamagishi, N., Callan, D. E., Goda, N., Anderson, S. J., Yoshida, Y., & Kawato, M. (2003). Attentional modulation of oscillatory activity in human visual cortex. *Neuroimage, 20,* 98–113.

Zeki, S. (1990). A century of cerebral achromatopsia. *Brain, 113,* 1721–1777.

Zhang, Y., & Ding, M. (2010). Detection of a weak somatosensory stimulus: Role of the prestimulus mu rhythm and its top–down modulation. *Journal of Cognitive Neuroscience, 22,* 307–322.